PLISKA
STUDIA MATHEMATICA

ПЛИСКА
МАТЕМАТИЧЕСКИ СТУДИИ

Pliska Stud. Math. **25** (2015), 119–128

PLISKA
STUDIA MATHEMATICA

MONITORING OF ADHESIVE JOINT USED IN LIGHTWEIGHT DEVICES*

T. Petrova, E. Kirilova, W. Becker, J. Ivanova

The excellent performance of the shear lag method for modeling smart pre-damaged bi-material structures under static and dynamic loading lies on the obtained important analytical formulae. The authors developed this method and applied it to investigate the piezoelectric response of a smart structure consisting in a piezoelectric patch over a host layer under static load and affected by electrical load at environment conditions. The interface delamination is investigated and the analytically calculated debond length is found, which is not considered in the typical local techniques. The numerical examples are oriented to the real materials used in the solar cells and other devices. The results are presented in figures and discussed in detail.

1. Introduction

Over the last decades, structural health monitoring has been recognized as a useful tool for improving the safety and reliability of structures [1]. Many monitoring techniques have been considered and developed in the literature [2, 3] in order to quantify and locate the damages in the lightweight structures [4]. These monitoring methods have their specific advantages for detecting damages in the structures. For example, in global dynamic techniques, it is well known that

*The authors greatly appreciate the financial support from the project BE 1090/40-1, 2015 of DFG, Germany.

2010 *Mathematics Subject Classification:* 74B15, 34A33.

Key words: smart structure, shear lag model, interface delamination, static and electric load, environmental conditions.

the structure is subjected to low-frequency excitations. Other typical local techniques, such as ultrasonic techniques, acoustic emission, and impact echo testing, require expensive and sophisticated hardware as well as well-trained professional operators.

On the other hand, electromechanical impedance based structural health monitoring has shown promising successes in monitoring and finding minor changes in structural integrity [5]. A key aspect of electromechanical impedance method is the use of piezoelectric patches as collocated sensors and actuators. To apply piezoelectric patches as an actuator-sensor simultaneously, a PZT patch bonded to a structure is driven by a fixed alternating electric field. Lim et al. [6] employed a new method for structural identification and damage detection using smart piezoelectric transducers.

Various FE models on piezoelectric structure interaction have been proposed since the 1990s. Lalande et al. [7] provided an excellent review about FE approaches for the simulation of piezoelectric patch–host structure interaction. Huang et al. [8] reviewed the development of analytical, numerical and hybrid approaches for modelling of the coupled piezo-elastodynamic behaviour. Therefore, it becomes an important issue to study the coupled electro-mechanical behaviour of these sensors with bonding layers to reliably evaluate the relation between the measured signal and the local mechanical deformation.

Encouraged by the excellent performance of the shear lag method for modelling smart pre-damaged bi-material structures and single lap joints [9] under mechanical loading at environmental conditions, the authors developed this method to investigate the piezoelectric response of the smart lightweight structures (piezoelectric patch over host layer) under static load and affected by electrical load at environment conditions. In the present paper the interface delamination of a patch from a substrate layer is under consideration and the analytically calculated interface debond length is found, which is not considered in the typical local techniques. Some criterion about the value of the electric gradient of the patch and detection of the corresponding interface debond length is formulated. The last result is of a big importance because such kind of lightweight structures is used as a basic element at solar panels, aircraft and other lightweight devices.

2. Statement of the problem

The shear lag method which started with the paper of Cox [10] for fiber-reinforced composites is now a common analytical tool in the engineering society. The shear lag hypothesis involves a simplification of in-plane shear stress and decouples the 2D problem into two 1D ones.

The following system of ordinary differential equations for a bi-material unit cell is obtained reducing the respective 2D case to a 1D case:

$$(1) \qquad \frac{d\sigma_A}{dx} - \frac{\tau_I}{2h_A} = 0 \quad \frac{d\sigma_B}{dx} + \frac{\tau_I}{2h_B} = 0 \quad \frac{dD_{zA}}{dz} = 0 \quad \frac{d^2T}{dx^2} = 0 \quad \frac{d^2H}{dx^2} = 0$$

It is assumed that the considered structure consists in the patch A which is piezoelectric and transversal isotropic, influenced by the temperature and electrical load and the layer B which is isotropic, but influenced from the temperature and moisture. The interface I is only isotropic. The considered structure is loaded by electrical load (patch A), mechanical strain load ε_0 along the axis $0x$ (layer B) and is influenced by temperature and moisture (see Figure 1). Following the goal of the present paper, the overlap zone $0 \le x \le l$ between the patch and layer will be taken into consideration (see Figure 1).

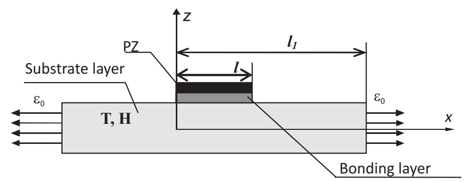

Figure 1: A representative unit solar cell

It is assumed that the kinematic behaviour within the structure is given by $\varepsilon_i^{tot} = \dfrac{du_i}{dx}$ and $\varepsilon_i^{mech} = \varepsilon^{tot} - \varepsilon_i^{pzel} - \varepsilon_i^{T} - \varepsilon_i^{H} \quad i = A, B, I$. According to the mechanical, electrical and environment conditions assumed above we have that for the interface I $\varepsilon_I^{pzel} = 0, \quad \varepsilon_I^{T} = 0, \quad \varepsilon_I^{H} = 0$, for the patch A $\varepsilon_I^{H} = 0$, while for the layer B $\varepsilon_i^{pzel} = 0$.

Mechanical, temperature and moisture boundary as well as mechanical contact conditions are:

$$\varepsilon_B(l) = \varepsilon_0 \quad \varepsilon_A(l) = 0$$

$$(2) \qquad \begin{array}{l} T_B(0) = T_0 \\ T_B(l) = T_1 \end{array} ; \quad \begin{array}{l} T_A(0) = T_0 \\ T_A(l) = T_1 \end{array} ; \quad \begin{array}{l} H_A(0) = H_0 \\ H_A(l) = H_1 \end{array} ; \quad \begin{array}{l} H_B(0) = H_0 \\ H_B(l) = H_1 \end{array}$$

where in (1, 2) $\sigma_\kappa, \ \varepsilon_k \quad (\kappa = A, B)$ are the mechanical stresses and strains, τ_I is the interfacial shear stress, D_{zA} is the electric displacement of patch A and H, T are the moisture concentration and temperature coming in the structure, respectively. The length and thickness of the patch and the layer are l and h_B, respectively. The width of the patch and layer are equal.

The integration of the last two equations of Eq(1) in the overlap zone gives the solutions : $T_A = T_1 - (T_1 - T_0)(1 - x/l)$, $T_B = T_1 - (T_1 - T_0)(1 - x/l)$; $H_A = H_1 - (H_1 - H_0)(1 - x/l)$, $H_B = H_1 - (H_1 - H_0)(1 - x/l)$.

So, the thermal and moisture strains are

$$
\begin{aligned}
&\varepsilon_i^T = \alpha_i\left[T_1 - (T_1 - T_0)(1 - \frac{x}{l})\right],\\
&\varepsilon_i^H = \beta_i\left[H_1 - (H_1 - H_0)(1 - \frac{x}{l})\right] \quad, (i = A,\, B)
\end{aligned} \tag{3}
$$

The solution $D_{zA} = D_0$, $0 \leq x \leq l$ of the third equation of (1) is obtained for the piezoelastic case [9], where D_{zA} is the electric displacement acting on the patch.

The constitutive equations for the patch A, layer B and for the interface I are given are in detail in [9]. We have:

$$
\begin{aligned}
&E_{zA} = \frac{D_{zA}}{\varepsilon_{33}^*} - \frac{p_3^*}{\varepsilon_{33}^*}\left[T_1 - (T_1 - T_0)(1 - \frac{x}{l})\right] - \frac{e_{31}^*}{\varepsilon_{33}^*}\frac{d\,u_A}{d\,x}\\
&\sigma_A = \left(c_{11}^* + \frac{e_{31}^{*2}}{\varepsilon_{33}^*}\right)\frac{d\,u_A}{d\,x} - \frac{e_{31}^*}{\varepsilon_{33}^*}D_0 - \left(\alpha_{11}^* - \frac{e_{31}^*}{\varepsilon_{33}^*}p_3^*\right)\left[T_1 - (T_1 - T_0)(1 - \frac{x}{l})\right]\\
&\sigma_x^B = \sigma_B = E_B\frac{d\,u_B}{d\,x} - E_B\alpha_B\left[T_1 - (T_1 - T_0)(1 - \frac{x}{l})\right]\\
&\qquad - E_B\beta_B\left[H_1 - (H_1 - H_0)(1 - \frac{x}{l})\right], \quad \tau_I = G_I\frac{u_A - u_B}{h_A + h_B}
\end{aligned} \tag{4}
$$

In (4) σ_κ and u_κ, $(\kappa = A,\, B)$ are mechanical stresses and displacements and E_{zA} is the electric gradient for patch A; c_{ij}, e_{ij}, ε_{ij}, α_{ij}, p_3 $(i, j = 1, 2, 3)$ are elastic constants (measured at constant electric field), piezoelectric and dielectric constants (measured at constant strain), thermal stress coefficients, pyroelectric coefficient for patch A; E_B, α_B, β_B are Young's modulus, thermal and moisture expansion coefficients for plate B and G_I is the shear modulus of the interface, respectively.

The problem will be solved in the selected overlap zone for the lightweight structure patch/layer, following the Volkersen procedure [11]. The following system of ordinary differential equations corresponds to the 1-D case within the shear lag hypothesis for the overlap zone of the patch A and the plate B:

$$
\frac{d\sigma_B}{dx} + \frac{\tau_I}{h_B} = 0, \quad \frac{d\sigma_A}{dx} - \frac{\tau_I}{h_A} = 0 \tag{5}
$$

According to Volkersen procedure the following condition for equilibrium has to be satisfied:

$$
\sigma_A h_A + \sigma_B h_B = \sigma_0 h_B \tag{6}
$$

where $\sigma_0 = E_B\varepsilon_0$ and ε_0 is the applied mechanical loading of type static extension to the plate B. At assumption that the widths of the patch and layer are equal, this condition follows from the equations (5).

Using (5/2) (4) and (6) the following ordinary differential equation for the axial stress σ_A is obtained:

$$\frac{d^2\sigma_A}{dx^2} - \lambda^2\sigma_A + B + Cx = 0, \qquad \lambda^2 = \frac{G_I}{h_I}\left(\frac{1}{E_A h_A} + \frac{1}{E_B h_B}\right)$$
$$B = \frac{G_I}{h_I h_A}\left\{\frac{\sigma_0}{E_B} - \left(\frac{D_A}{E_A} - \frac{D_B}{E_B}\right) - \left(\frac{T_{1A}}{E_A} - \frac{T_{1B}}{E_B}\right) - \left(\frac{H_{1A}}{E_A} - \frac{H_{1B}}{E_B}\right)\right\}$$
$$C = -\frac{G_I}{h_I h_A}\left\{\left(\frac{T_{2A}}{E_A} - \frac{T_{2B}}{E_B}\right) + \left(\frac{H_{2A}}{E_A} - \frac{H_{2B}}{E_B}\right)\right\}$$

The system of equations (5) has to satisfy the following boundary conditions:

(7) $$\sigma_A(0) = 0 \quad \sigma_A(l) = 0$$

The solution of (5/1) has the form:

$$\sigma_A = \frac{1}{\lambda^2 sh(\lambda l)}\left\{-Bsh[\lambda(l-x)] - (B+Cl)\,sh(\lambda x) + (B+Cx)\,sh(\lambda l)\right\}.$$

The total hygrothermalpiezoelastic stresses and electric gradient for the model (Figure 1) in the overlap zone read:

$$\sigma_A = \frac{1}{\lambda^2 sh(\lambda l)}\left\{-Bsh[\lambda(l-x)] - (B+Cl)\,sh(\lambda x) + (B+Cx)\,sh(\lambda l)\right\}$$

(8) $$\sigma_B = E_B\varepsilon_0 - \frac{h_A\left\{-Bsh[\lambda(l-x)] - (B+Cl)\,sh(\lambda x) + (B+Cx)\,sh(\lambda l)\right\}}{\lambda^2 h_B sh(\lambda l)}$$

$$\tau_I = \frac{h_A}{\lambda sh(\lambda l)}\left\{Bch[\lambda(l-x) - (B+Cl)\,ch(\lambda x) + C\frac{sh(\lambda l)}{\lambda}\right\}$$

$$E_{zA} = (D_{zA})/(\varepsilon_{33}^*) - (p_3^*)/(\varepsilon_{33}^*)\left[T_1 - (T_1 - T_0)(1 - \frac{x}{l})\right] - (e_{31}^*)/(\varepsilon_{33}^*)(\sigma_A)/(E_A)$$

The length of an interfacial debonding is found from the condition that the interface shear stress reaches its failure limit τ^{cr}, i.e. $\tau_I(l_e) = \tau^{cr}$. Accordingly we have the following equation to be solved with respect to the debond length l_e:

(9) $$\tau_I = \frac{h_A}{\lambda sh(\lambda l)}\left\{Bch[\lambda(l-x) - (B+Cl)\,ch(\lambda x) + C\frac{sh(\lambda l)}{\lambda}\right\}$$

So, we get:

(10) $$\tau_I(l_e) = \frac{h_A}{\lambda sh(\lambda l)}\left\{Bch[\lambda(l-l_e) - (B+Cl)\,ch(\lambda l_e) + C\frac{sh(\lambda l)}{\lambda}\right\} = \tau^{cr}$$

The substitution $\exp(\lambda l_e) = y$ in (10) leads to the following quadratic algebraic equation:

$$Py^2 - 2Qy + R = 0, \quad \text{where} \tag{11}$$

$$Py^2 - 2Qy + R = 0, \quad P = B\left[ch(\lambda l) - sh(\lambda l)\right] + \left(\frac{P\lambda^2}{wh_A} - B - Cl\right)$$

$$Q = sh(\lambda l)\left(\frac{\lambda\tau^{cr}}{h_A} - \frac{C}{\lambda}\right), \quad R = B\left[ch(\lambda l) + sh(\lambda l)\right] + \left(\frac{P\lambda^2}{wh_A} - B - Cl\right)$$

The roots of (11) are found as $y_{1,2} = \dfrac{Q \pm \sqrt{Q^2 - PR}}{P}$, so the debond interface length according to the above written substitution is $l_e = \dfrac{1}{\lambda} \ln \dfrac{Q \pm \sqrt{Q^2 - PR}}{P}$. We look for a positive debond length, so the logarithmic argument must be greater or equal to 1, i.e., $\dfrac{Q \pm \sqrt{Q^2 - PR}}{P} \geq 1$.

3. Numerical examples

Three examples will be considered. First of them case 1 (Cu/Si) is connected with a modeling of an ordinary unit solar cell, the second case 2 (PZT-5H/CFRP) [12] and the third case 3 (PZT-4/IM7 8852) [9] are directed to another smart lightweight structure patch/layer with application in automotive industry. For this purpose in Table 1 the mechanical and physical properties of the used material are given. $h_A = 1$ mm; $h_B = 2$ mm; $\varepsilon_0 = 0.1\% \div 2\%$; $l = 50$ mm; $D_0 = 0.055$ C/m^2; $G_I = 800$ MPa; $\tau^{cr} = 18$ MPa; $T_0 = 263 \div 273$ K; $T_1 = 293 \div 333$ K; $H_0 = 0.05 \div 5(\%)$; $H_1 = 5.0 \div 40(\%)$

Case 1

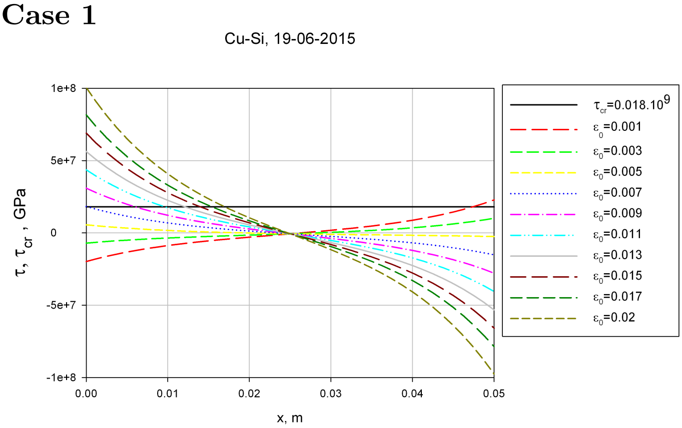

Figure 2: Interface shear stress for patch (Cu)/ layer (Si) along the overlap zone

Case 2

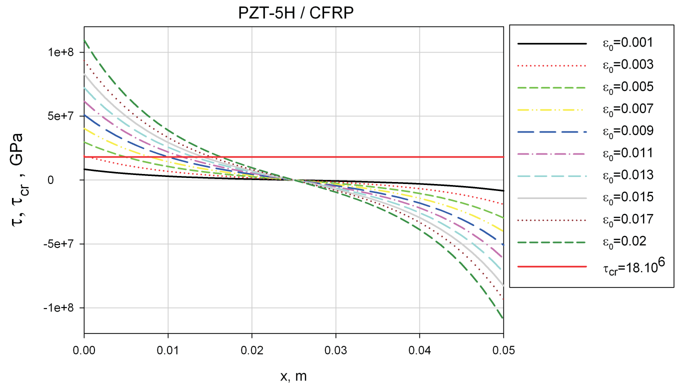

Figure 3: Interface shear stress for patch (PZT-5H)/ layer (CFRP) along the overlap zone

Case 1, 2, 3

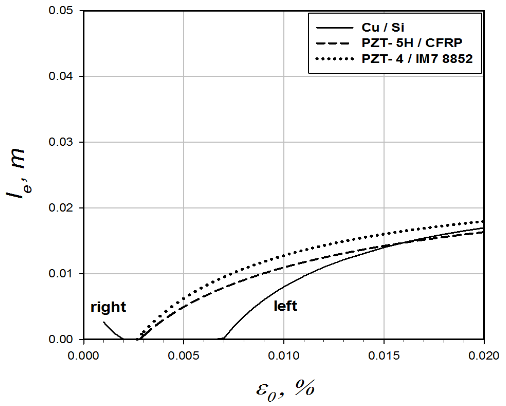

Figure 4: Interface debond length for case 1 Cu/ Si, case 2 PZT-5H/CFRP, case 3 PZT-4/IM7 8852 for different values of the static load

Case 2 and 3

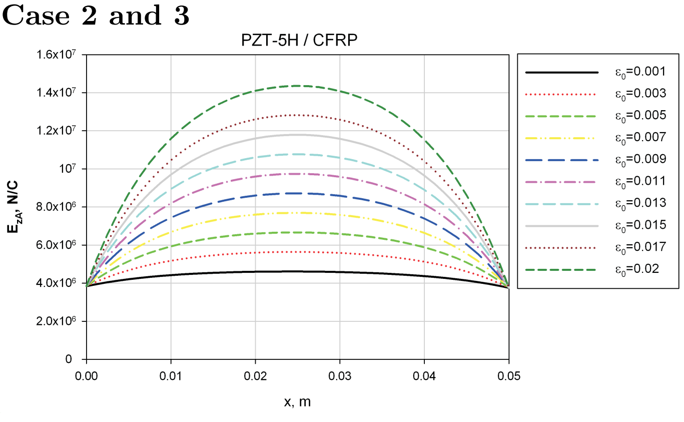

Figure 5: Electric gradient for patch (PZT-5H)/ layer (CFRP) along the overlap zone

Case 3. The behavior of the shear stress along the overlap zone is quite similar to PZT-5H/CFRP and is not shown here.

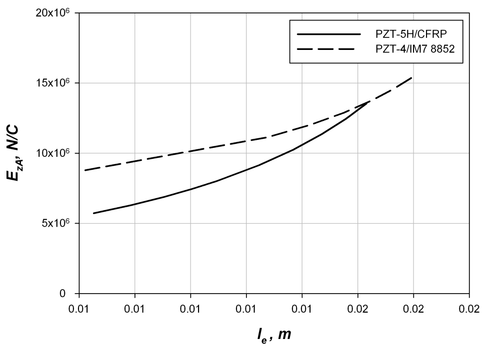

Figure 6: Indirect dependence of the electric gradient on debond length for (PZT-4)/(IM78552) and (PZT-5H)/(CFRP) at fixed value of static and physical loading

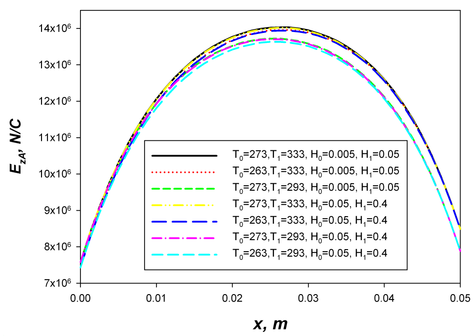

Figure 7: Dependence of the electric gradient on temperature and moisture concentration at fixed static load $\varepsilon_0 = 0.015$, case 3

Figures 2 and 3 describe the behavior of the interface shear stress along the axis $0x$ in the overlap zones for the considered 3 cases. The presence of the electric load (Fig. 3) seriously changes the interface delamination for these structures (case 2, 3), detaining the delamination from the right end of the patch, while for the case 1 (Fig. 2) the delamination from the both ends of the patch arises. The straight line $\tau(l_e) = \tau^{cr}$ intersects the shear stress, showing graphically the places of the interface delamination. Let denote the interface delamination starting from origin of the axis $0x$ as l_{left} (left) and from the end of the overlap zone as l_{right} (right), respectively.

Figure 4 illustrates the behavior of the interface debond length as a function of the static load for the cases 1, 2, 3 respectively. It can be seen that the interface debond length is a monotonically increasing function of the static load at constant values of the electrical displacement and temperature and moisture concentration. For the three considered cases the full degradation of the interface is not reached.

In Figure 5 the behavior of the electric gradient along the length of the overlap zone at different values of the static loading and for fixed temperature and moisture concentration (cases 2 and 3) is shown. Increasing the static load the electric gradient increases as well, reaching the maximal value at the half of the overlap zone. The behavior of the structure PZT 4/IM7 8852 is quite similar.

The indirect dependence of the electric gradient and interface debond length is shown in Figures 6 for cases 2 and 3. These dependences show that to the given value of the electric gradient the respective unique value of the debond length corresponds and could be regarded as a possible criterion for detecting the length of the interface debonding via the respective value of the electric gradient.

The influence of the temperature load and moisture concentration for case 3 is shown in Fig. 7. It is seen, that the value of the temperature T_1 definitely influences the electric gradient $E_{zA}(x)$ and the axial stress $\sigma_A(x)$ as well. The decreasing of the value of T_1 decreases the electric gradient and reflects on the value of debond length. Similar, but weaker influence on the value of $E_{zA}(x)$ is observed when T_0 decreases. Changes in the moisture concentrations do not influence value of electric gradient for considered materials.

4. Conclusions

The lightweight structure patch/layer is a subject under consideration in the present paper. On the structure the combined load is applied consisting in static mechanical and electric load at temperature and moisture exposure. The shear lag model is used to determine the behavior of the interface shear stress and interface debond length. Three structures are considered: two of them are supposed to be smart ones, while the third is an ordinary unit solar cell without piezo properties.

From the analysis provided the following conclusions can be made:

- The piezo properties and electrical load significantly influence the initiation of the left side interface delamination in the overlap zone and preserve the patch from the right side interface delamination
- The influence of the moisture and temperature coming to the structures are expressed by detaining the interface delamination
- The indirect dependence cam be summarized to the conclusion that to the value of the electric gradient the unique value of debond length corresponds and can be used to give the expected value for the interface debond length.

REFERENCES

[1] S. Park, C.-B. Yun, Y. Roh, and J.-J. Lee. PZT-based active damage detection techniques for steel bridge components. *Smart Materials and Structures*, **15**, *4* (2006), 957–966.

[2] R. D. Adams, P. Cawley, C. J. Pye, B. J. Stone. A vibration testing for non-destructively assessing the integrity of the structures. *Journal of Mechanical Engineering Science*, **20**, *2* (1978), 93–100.

[3] P. Tan, L. Tong. Identification of delamination in a composite beam using integrated piezoelectric sensor/actuator layer. *Composite Structures*, **66**, *1–4* (2004), 391–398.

[4] S. Bhalla, C. K. Soh. High frequency piezoelectric signatures for diagnosis of seismic/blast induced structural damages. *NDT and E International*, **37**, *1* (2004), 23–33.

[5] V. Giurgiutiu, A. Reynolds, C. A. Rogers. Experimental investigation of E/M impedance health monitoring for spot welded structural joints. *Journal of Intelligent Material Systems and Structures*, **10**, *10* (1999), 802–812.

[6] Y. Y. Lim, S. Bhalla, C. K. Soh. Structural identification and damage diagnosis using self-sensing piezo-impedance transducers. *Smart Materials and Structures*, **15**, *4* (2006), 987–995.

[7] F. Lalande, Z. Chaudhry, C. A. Rogers. Impedance-based modelling of actuators bonded to shell structures. *J. Intelligent Mater. Syst. Struct.*, **6** (1995), 765–774.

[8] G. Huang, F. Song, X. Wang. Quantitative modelling of coupled piezo-elasto dynamic behaviour of piezoelectric actuators bonded to an elastic medium for structural health monitoring: a review. *Sensors*, **10** (2010), 3681–3702.

[9] W. Becker, V. Valeva, T. Petrova, J. Ivanova. Monitoring of piezo single lap joints under static loading, SDEWES2014-0202, In: Proc. 9$^{\text{th}}$ Conf. on Sustainable Development of Energy, Water and Environment Systems – SDEWES, 20–27 September 2014, Venice-Venice, 2014, CD.

[10] L. H. Cox. The Elasticity and Strength of Paper and Other Fibrous Materials. *Brit. J. Appl. Phys.*, **3**, *3* (1952), 2–79.

[11] O. Volkersen. *Luftfahrtforschung*, **15** (1938), 41–47

[12] W. Becker, V. Valeva, T. Petrova, J. Ivanova. Technical Damage in Wind Rotor Blade under Static Load at Environment Conditions. *Chemical Engineering Transactions*, **42** (2014), 91–96.

T. Petrova, E. Kirilova
Institute of chemical Engineering
BAS, Sofia, Bulgaria

W. Becker
University of Darmstadt
Darmstadt, Germany

J. Ivanova
Institute of Mechanics
BAS, Sofia, Bulgaria
e-mail: `ivanova@imbm.bas.bg`